Proceedings of the
Annual Stability Conference
Structural Stability Research Council
Atlanta, Georgia, April 21-24, 2026

Optimization and sensitivity analysis in buckling problems

Nuno Peres[1], Rodrigo Gonçalves[2]

Abstract
This paper discusses optimization in the context of finding the minimum critical bifurcation load in elastic structures subjected to several (possibly many) load combinations. This has practical relevance in worst-case scenario analysis and stability-aware design verification. Two problems are addressed. In the first problem it is assumed that the individual load case magnitudes can vary continuously while satisfying certain constraints, in which case the minimum can be found using a gradient-based approach with closest-point projection to the constraint hypersurface. Moreover, it is shown that the gradient of eigenvalues makes it possible to identify the most buckling-sensitive members in structures. In the second problem the load case magnitudes assume discrete values, as in typical limit state load combinations, thus motivating the use of a Genetic Algorithm. To show the capabilities of the proposed approaches, a few numerical examples are presented, mainly concerning 2D frames buckling in in-plane modes, even if thin-walled lipped channel members buckling in distortional and local modes are also addressed.

1. Introduction

Optimization seeks to find the best solution for a given set of variables which are subject to given constraints. In the particular case of the structural optimization of steel frames, common strategies involve optimizing total weight or specific features, by changing the geometry and the distribution of mass and stiffness, given a set of loads and their combination rules, as well as additional constraints (e.g. Saka 2007, Togan 2012, Murren & Khandelwal 2014, Ye et al. 2016, Gholizadeh et al. 2020, Neves et al. 2024). This paper addresses an intermediate practical problem, which consists of finding the load combination that minimizes the critical bifurcation load of a given structure, subjected to several (possibly many) load cases and their combination rules. Consequently, the load cases are treated as design variables, and the objective is to identify their combination that minimizes the critical bifurcation load while satisfying prescribed admissibility constraints. This problem is of interest when many load combinations are possible, in which case the evaluation of the worst-case scenario using an exhaustive (brute-force) search can be computationally expensive, and to draw meaningful conclusions concerning the stability behavior of the structure. Moreover, a fast identification of the most detrimental load combination can

[1] Assistant Researcher, Laboratório Nacional de Engenharia Civil (LNEC), Portugal <nperes@lnec.pt>
[2] Full Professor, CERIS and Universidade Nova de Lisboa, Portugal <rodrigo.goncalves@fct.unl.pt>

improve the computational burden of a higher-order structural optimization. As explained next, two distinct problems are considered.

In the first problem the individual load case magnitudes vary continuously and satisfy a certain prescribed constraint, expressed as a norm or linear combination, defining a hypersurface in load magnitude space. In this case the minimum critical load is sought using a specifically tailored gradient-based search technique with closest-point projection. The gradient defines the sensitivities of the critical eigenvalue with respect to the magnitudes and allows identifying the directions that are most detrimental to stability. Moreover, sensitivities also make it possible to determine the member or component that exerts the greatest influence on the system critical load.

In the second problem, the load case magnitudes can only assume a finite set of discrete values, as commonly encountered in limit state design using code-prescribed load combinations. The resulting minimization problem is combinatorial in nature and generally non-smooth, making gradient-based approaches unsuitable. To address this case, a Genetic Algorithm is employed, enabling an efficient exploration of the discrete load space and the identification of the minimum bifurcation load.

For illustrative purposes, a set of numerical examples is presented and discussed. These examples involve 2D frame structures and lipped channel columns buckling in distortional/local modes, and illustrate how both continuous and discrete minimum-finding strategies can be used to reveal worst-case loading scenarios. Moreover, it is shown how the proposed procedures can identify buckling-sensitive members.

2. Mathematical preliminaries

Consider an elastic structure undergoing negligible pre-buckling deflections and discretized by the finite element method. The linearized buckling eigenvalue problem assumes the standard form

$$(\mathbf{K} + \lambda\mathbf{G})\mathbf{v} = \mathbf{0}, \tag{1}$$

where throughout the paper bold symbols denote matrices and vectors, $\mathbf{K}$ is the symmetric positive definite linear stiffness matrix, $\mathbf{G}$ is the symmetric geometric stiffness matrix, λ is the load parameter and $\mathbf{v}$ is the vector of nodal DOFs. The nontrivial solutions provide the bifurcation loads λ (eigenvalues) and corresponding buckling modes $\mathbf{v}$ (eigenvectors). The critical bifurcation load corresponds to the minimum positive eigenvalue; negative eigenvalues are herein assumed inadmissible.

It can be shown that the derivative of a simple (multiplicity = 1) eigenvalue λ_i, with respect to some parameter α_j, reads (e.g. Courant and Hilbert 1953, Wittrick 1962)

$$\frac{\partial\lambda_i}{\partial\alpha_j} = \frac{1}{\mathbf{v}_i^{\mathrm{T}}\mathbf{G}\mathbf{v}_i}\mathbf{v}_i^{\mathrm{T}}\left(\frac{\partial\mathbf{K}}{\partial\alpha_j} - \lambda_i\frac{\partial\mathbf{G}}{\partial\alpha_j}\right)\mathbf{v}_i, \tag{2}$$

where $\mathbf{v}_i$ is the eigenvector associated with the eigenvalue λ_i.

Of interest to this work is the particular case of the derivative with respect to the loading. Consider that the loads correspond to a superposition of $j = 1, \dots, D$ load patterns or cases. According to the linear stability analysis concept, a linear prebuckling stress state is assumed and therefore the geometric stiffness matrix can be decomposed as

$$\mathbf{G} = \sum_{j=1}^{D} \alpha_j \mathbf{G}_j, \tag{3}$$

where α_j is the scalar load weight or magnitude, always assumed positive, pertaining to load case j, and $\mathbf{G}_j$ is the corresponding geometric matrix. The derivative of the linear stiffness matrix is null and one obtains

$$\frac{\partial \lambda_i}{\partial \alpha_j} = \frac{\lambda_i}{\mathbf{v}_i^{\mathrm{T}} \mathbf{G} \mathbf{v}_i} g_j, \quad \text{with} \quad g_j = -\mathbf{v}_i^{\mathrm{T}} \mathbf{G}_j \mathbf{v}_i. \tag{4}$$

The sensitivity to each parameter is provided by g_j and the gradient reads (the subscript i is dropped for simplicity)

$$\nabla \lambda = \frac{\lambda}{\mathbf{v}^{\mathrm{T}} \mathbf{G} \mathbf{v}} \boldsymbol{g}, \qquad \boldsymbol{g} = \begin{bmatrix} g_1 \\ \vdots \\ g_D \end{bmatrix}. \tag{5}$$

The problem addressed in this work thus corresponds to finding

$$\min_{\boldsymbol{\alpha}} \lambda_{min} \left(\mathbf{K}, \mathbf{G}(\boldsymbol{\alpha}) \right), \tag{6}$$

associated with the eigenvalue problem (1) and subjected to some constraints on vector $\boldsymbol{\alpha}$ (collecting the load case magnitudes α_j). In the following, the subscript $(\cdot)_{min}$ is omitted when no ambiguity exists, for simplicity.

The eigenvalue sensitivities provide not only the gradient for minimum-seeking purposes, but also a physically meaningful measure of how strongly each load case influences the stability of the structure. This motivates the definition of the structure "critical" member for a given loading: *the member for which the sensitivity of the minimum eigenvalue with respect to some parameter (geometric, material or loading) is the highest*. In other words, the member that exerts the greatest influence on the structure critical bifurcation load (according to the chosen parameter). For the sensitivity to geometric or material parameters, the general Eq. (2) must be used. For the sensitivity with respect to each member loading, it must be assumed that it is possible to find (exactly or approximately) a decomposition in the form of Eq. (3), where each load case *j* introduces stresses only in member *j*. From Eq. (4), the "critical" member is the one with the highest g_k value.

3. The continuous case

Consider first the case where all α_j can vary continuously and satisfy the constraints

$$f(\boldsymbol{\alpha}) = 0, \quad 0 \leq \alpha_j \leq 1, \tag{7}$$

where the first condition defines a smooth hypersurface in load space. The minimum is found as explained next and illustrated in Fig. 1(a), which for simplicity shows the 2D case. Each level set $\lambda = \text{constant}$ corresponds to a hypersurface (an isoline curve in the figure) and two level sets A and B satisfy the scaling property $\lambda^B/\lambda^A = \alpha_j^A/\alpha_j^B$. Furthermore, λ increases moving towards the origin.

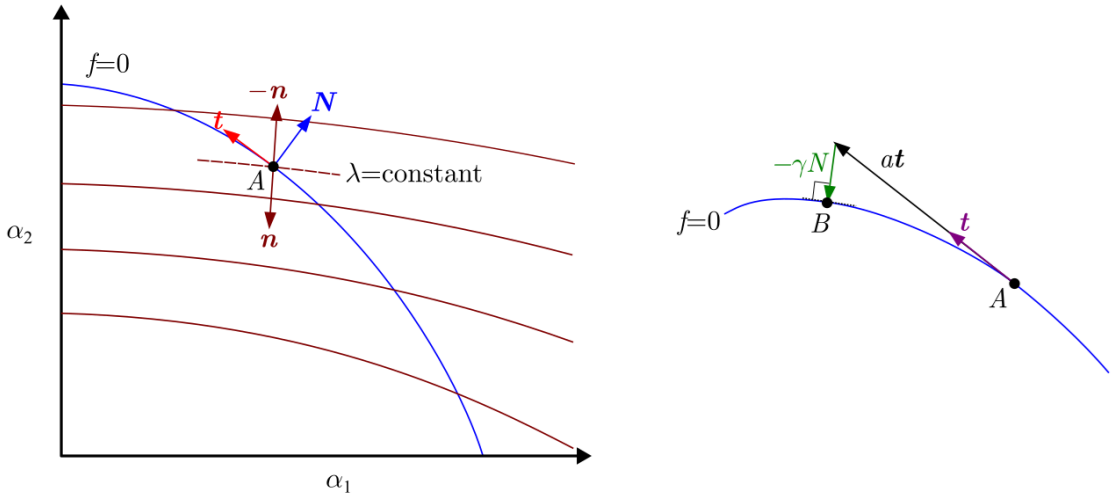

(a) (b)

Figure 1: Minimum-finding procedure for the continuous case: (a) search direction $\boldsymbol{t}$ and (b) closest-point projection

The minimum load parameter is found starting from a given trial point A on $f = 0$, see Fig. 1(a). The normal to the level set is calculated from

$$\boldsymbol{n} = \frac{\nabla\lambda}{\|\nabla\lambda\|}. \tag{8}$$

The search direction for the minimum corresponds to the steepest descent, following the tangent $\boldsymbol{t}$ closest to $-\boldsymbol{n}$, thus corresponding to the projection of $\boldsymbol{n}$ on the tangent plane to the level set, viz.

$$\begin{cases} \boldsymbol{t} = \frac{\boldsymbol{d}}{\|\boldsymbol{d}\|} \\ \boldsymbol{d} = (\boldsymbol{n}\cdot\boldsymbol{N})\boldsymbol{N} - \boldsymbol{n} = (\boldsymbol{N}\otimes\boldsymbol{N} - \mathbf{I})\boldsymbol{n} \\ \boldsymbol{N} = \frac{\nabla f}{\|\nabla f\|} \end{cases} \tag{9}$$

where $\mathbf{I}$ is the identity matrix and $\otimes$ denotes the standard tensor product between two vectors. The next trial point B is calculated using a suitable scalar a and performing a closest-point projection using the Backward Euler scheme, with (see Fig. 1 (b))

$$\begin{cases} f(\boldsymbol{\alpha}_B) = 0 \\ \boldsymbol{r} = \boldsymbol{\alpha}_B - (\boldsymbol{\alpha}_A + a\boldsymbol{t} - \gamma\boldsymbol{N}) = \mathbf{0} \end{cases} \tag{10}$$

which requires Newton-Raphson iterations to obtain γ, using the increment

$$\Delta\gamma = \frac{f - \nabla f^{\mathrm{T}}(\mathbf{I}+\gamma\nabla\boldsymbol{N})^{-1}\boldsymbol{r}}{\nabla f^{\mathrm{T}}(\mathbf{I}+\gamma\nabla\boldsymbol{N})^{-1}\boldsymbol{N}}. \tag{11}$$

The critical load is evaluated at the new point B and also at intermediate points (by setting appropriate intermediate values for a), following a line search strategy. If $\boldsymbol{at}$ lies outside the search space, it is truncated to meet the bound criteria. The procedure converges quite rapidly and provides direct insight into the most unfavorable directions in load space.

4. The discrete case

In limit state load combinations prescribed by design codes, α_k assume discrete values and typically one load case is set as "leading", assuming a higher magnitude. In this case the admissible set is finite and combinatorial, thus the bifurcation loads become non-smooth function of the load case magnitudes. A Genetic Algorithm is well suited to solve the problem efficiently. Although computationally demanding, this strategy is well suited to explore large discrete load spaces with complex constraints.

For a D-dimensional load space, D+1 parameters are encoded in each "chromosome":

(i) D regular "genes" having binary values {0, 1}, with 0 when the load is absent (e.g. live loads) or beneficial (e.g. beneficial self-weight) and 1 when it acts with its combination value;

(ii) a single gene (D+1) that controls the leading loading. This gene can assume several values {0, 1, …, D}, where a null value indicates that no loading is leading, while a non-null integer specifies the leading loading, overriding the information encoded in the corresponding gene. The mutation of this gene must have the same probability for all integers.

The algorithm is initialized by creating a population of P individuals, each with a chromosome generated uniformly sampling from $\{0, 1\}^D$ for the regular genes and from {0, 1, …, D} for the leading-loading gene. After initialization, the fitness of each individual is evaluated by decoding the chromosome into the corresponding load combination and performing a linear stability analysis. The smallest positive bifurcation load factor is adopted as the fitness value.

The algorithm proceeds iteratively as follows:

1. At each generation, individuals are ranked according to their fitness and a small number of the best solutions is preserved unchanged ("elitism") to prevent the loss of the most critical load combinations found so far.
2. The remaining individuals of the next generation are created through a stochastic "reproduction" process. Parent chromosomes are selected using "tournament selection", which biases reproduction toward fitter individuals while maintaining population diversity. In this procedure, t individuals are randomly sampled from the population and the one with the best fitness is selected as parent; the process is repeated to select a second parent.
3. New offspring are generated by "crossover", combining the information carried by the regular genes and the leading-loading gene of the two parents. The leading-loading gene of the offspring is inherited from either parent with equal probability, while the regular genes are combined by uniform crossover.
4. To promote exploration of the discrete admissible set and avoid premature convergence, a "mutation" operation is carried out. Mutation consists of random bit flips of the regular genes

and random reassignment of the leading-loading gene, ensuring equal probability for all admissible leading-loading cases. The mutation probabilities are chosen to be sufficiently small to preserve good solutions while maintaining exploration.

5. The new population is formed by combining the elite individuals and the newly generated offspring, maintaining a constant population size.

The process is repeated over successive generations until convergence is achieved, either when a prescribed maximum number of generations is reached or when the best fitness value does not improve over a given number of generations. The final solution corresponds to the load combination associated with the minimum critical bifurcation load factor encountered during the search.

5. Numerical examples

Several numerical examples are presented in this section, to illustrate the application of the proposed methodologies, for both the continuous and discrete cases. Moreover, the "critical" member concept is also exemplified.

The finite element and minimum-finding procedures were implemented in MATLAB (2024). It should be mentioned that these procedures are quite fast. Using an AMD Ryzen 7 7840HS w/ Radeon 780M Graphics (3.80 GHz), the runtimes were as follows (i) 1.5 seconds for each graph in Fig. 3, calculated with approximately 10,000 points, (ii) 0.07 seconds for each for the example in Section 5.4 and (iii) 0.1 seconds for the example in Section 5.5 concerning the application of the Genetic Algorithm.

5.1 The 2D beam-column finite element

Most of the examples concern 2D frames and are solved using a standard Euler-Bernoulli finite element with Hermite cubic interpolation for the transverse displacements and linear Lagrange interpolation for the axial displacements. The finite element linear and geometric stiffness matrices read (e.g. Przemieniecki 1968)

$$\mathbf{K}_e = \frac{EI}{L}\begin{bmatrix} A/I & 0 & 0 & -A/I & 0 & 0 \\ & \frac{12}{L^2} & 6/L & 0 & -\frac{12}{L^2} & 6/L \\ & & 4 & 0 & -6/L & 2 \\ & & & A/I & 0 & 0 \\ & & & & \frac{12}{L^2} & -6/L \\ \text{Sym.} & & & & & 4 \end{bmatrix}, \quad \mathbf{G}_e = \frac{N}{30L}\begin{bmatrix} 0 & 0 & 0 & 0 & 0 & 0 \\ & 36 & 3L & 0 & -36 & 3L \\ & & 4L^2 & 0 & -3L & -L^2 \\ & & & 0 & 0 & 0 \\ & & & & 36 & -3L \\ \text{Sym.} & & & & & 4L^2 \end{bmatrix}, \quad (12)$$

for the DOF vector $\mathbf{d}^{\mathrm{T}} = [u_1 \quad w_1 \quad \theta_1 \quad u_2 \quad w_2 \quad \theta_2]$, where E is Young's modulus, A is the cross-section area, I is the cross-section second moment of area, L is the element length and N is the axial force, negative for compression. In the examples, each bar is discretized using three equal length finite elements.

5.2 "Critical" member in a frame

To illustrate the determination of the "critical" member, consider the frame shown in Fig. 2. The sensitivity of the eigenvalue is calculated with respect to the axial forces, subdividing the load as α_1 and α_2. Furthermore, the sensitivity with respect to the second moment of area is also evaluated, using

$$\frac{\partial \lambda_i}{\partial I_j} = \frac{1}{\mathbf{v}_i^{\mathrm{T}} \mathbf{G} \mathbf{v}_i} k_j, \quad \text{with} \quad k_j = \mathbf{v}_i^{\mathrm{T}} \frac{\partial \mathbf{K}_j}{\partial I_j} \mathbf{v}_i \quad \text{and} \quad \mathbf{K} = \sum_{j=1}^{D} \mathbf{K}_j \tag{13}$$

where the derivative of the linear stiffness matrix is null except for member j, hence the computation of k_j is restricted to that member (as in the calculation of g_j).

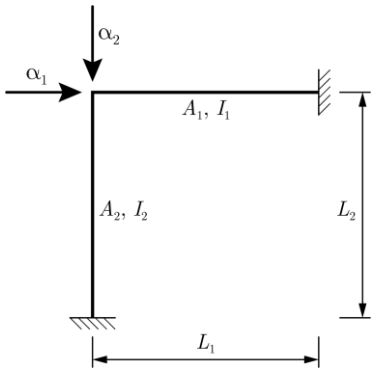

Figure 2: Inverted L-frame

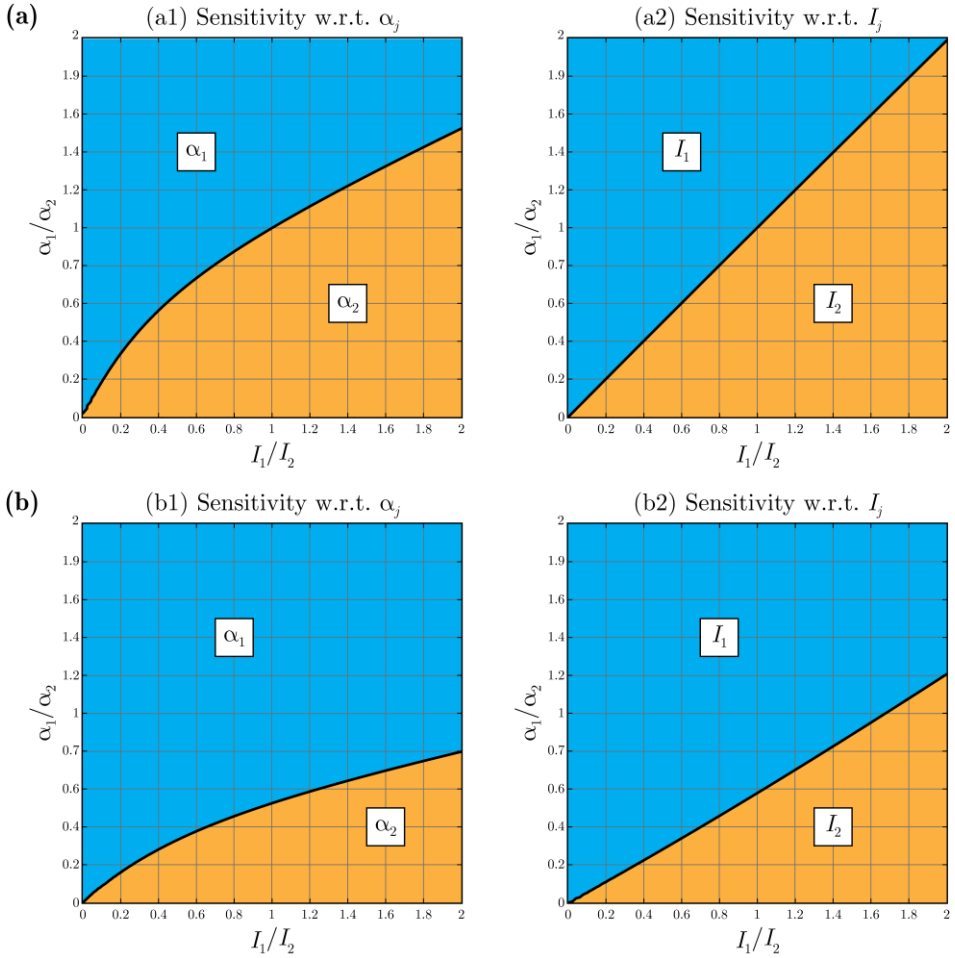

Figure 3: Sensitivities with respect to α_j and I_j for (a) $L_1 = L_2$ and (b) $L_1 = 1.5L_2$

The sensitivities with respect to α_j and to I_j $(j = 1, 2)$ were calculated by varying α_1/α_2 and I_1/I_2 between 0 and 2. Figs. 3 show the parameter domain subdivided into colored regions indicating where the influence of each variable is dominant, as well as the boundary separating these regions, at which their influences are equal. The results are presented for (a) $L_1 = L_2$ and (b) $L_1 = 1.5L_2$.

For case (a) both boundaries pass through point (1,1), since geometric and loading symmetry hold. However, the boundary is non-linear for the sensitivity with respect to the loading, while it is linear for I_j — recall that the former is calculated with Eq. (4) and depends on the geometric matrix, while the latter is obtained from Eq. (13) and depends on the linear matrix. It is also worth noting that, for both boundaries, if a point (x, y) lies on the boundary, so does $(1/x, 1/y)$, since the inversion corresponds to swapping the axial force and the second moment of area of members 1 and 2. Case (b) retains some similarities with case (a), but the boundaries no longer pass through point (1,1) and the inversion relation does not hold.

5.3 "Critical" wall in a lipped channel column

The "critical" member concept can be applied to the walls of a thin-walled member undergoing local or distortional buckling. A very efficient approach can be followed if a single Generalized Beam Theory — GBT, see the latest developments described in Gonçalves et al. (2023) — deformation mode is used as a Ritz-like approximation of the buckling mode. In this case the minimum critical load (calculated for the appropriate half-wavelength) has the analytical solution (Schardt, 1994)

$$\lambda = -\frac{\mathsf{D}_{kk}+2\sqrt{\mathsf{C}_{kk}\mathsf{B}_{kk}}}{\mathsf{X}_{kk}}, \tag{14}$$

where B_{kk}, C_{kk}, D_{kk} are the GBT linear modal matrix components pertaining to deformation mode *k*, while X_{kk} is the geometric counterpart. The derivative with respect to the geometric term yields

$$\frac{\partial\lambda}{\partial\alpha_j} = \frac{\mathsf{D}_{kk}+2\sqrt{\mathsf{C}_{kk}\mathsf{B}_{kk}}}{\mathsf{X}_{kk}^2}\frac{\partial\mathsf{X}_{kk}}{\partial\alpha_j} = -\frac{\lambda}{\mathsf{X}_{kk}}\frac{\partial\mathsf{X}_{kk}}{\partial\alpha_j}, \tag{15}$$

and coincides with Eq. (2) for the scalar case.

To obtain the derivatives, it is assumed that the geometric term can be decomposed according to

$$\mathsf{X}_{kk} = \sum_{j=1}^{D}\alpha_j(\mathsf{X}_{kk})_j, \tag{16}$$

where *j* indicates the wall number and it is assumed, as a first approximation, that it is possible to apply independent compression to each wall. The sensitivity therefore only depends on

$$g_j = -\frac{\partial\mathsf{X}_{kk}}{\partial\alpha_j} = -(\mathsf{X}_{kk})_j. \tag{17}$$

Consequently, the procedure only requires calculation of the relevant deformation modes, using GBTUL (Bebiano et al. 2015, 2018), freely downloadable from https://sites.fct.unl.pt/gbt/, and the computation of the geometric terms for each wall j,

$$(\mathsf{X}_{kk})_j = -t \int_0^{b_j} (\bar{v}_k^2 + \bar{w}_k^2)\, \mathrm{d}y, \tag{18}$$

where b_j is the width of the wall (y is the corresponding coordinate), t is the wall thickness, $\bar{v}_k$, $\bar{w}_k$ are the mid-line (along y) and transverse displacements pertaining to deformation mode k, and a uniform unit compressive stress distribution was assumed.

Fig. 4 shows two lipped channel sections, as well as the deformation modes considered: 5 (symmetric distortion) and 7 (first local-plate). Table 1 displays the normalized sensitivity coefficients g_j/g_{max}, for each cross-section and deformation mode. For the calculation of the GBT deformation modes, a cross-section discretization using 3 intermediate nodes in the web and 2 in each flange was adopted. The results in the table make it possible to conclude that the flange is always critical for distortional buckling, whereas for local buckling the web is critical in Case 1, while the flange is critical for Case 2 (closely followed by the web, since the walls have the same width).

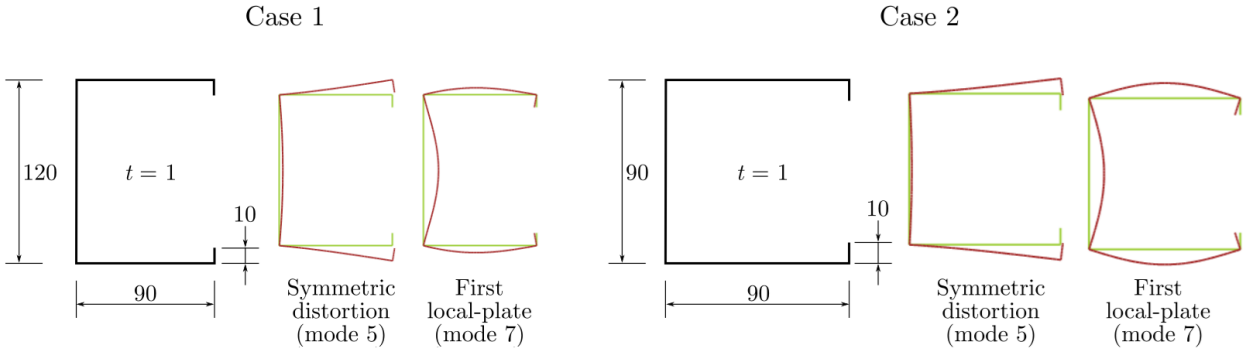

Figure 4: Lipped channel geometries and GBT deformation modes 5 and 7

Table 1: Normalized sensitivity coefficients g_j/g_{max} for lipped channel columns

	Case 1		Case 2	
	Distortional	Local	Distortional	Local
Lip	0.38	0.001	0.39	0.01
flange	1.00	0.17	1.00	1.00
web	0.14	1.00	0.05	0.99

5.4 Inverted L-frame

The minimum-finding procedure introduced in Section 3 for the continuous case was applied to the inverted L-frame shown in Fig. 2. Both members have equal length (thus $L_1 = L_2$) and Young's modulus $E = 210$ GPa, but the cross-sections are different. The horizontal bar has a HEB120 cross-section ($A_1 = 34$ cm^2, $I_1 = 317.5$ cm^4) whereas the vertical bar has a HEB100 cross-section ($A_2 = 26$ cm^2, $I_2 = 167.3$ cm^4). A p-norm constraint is enforced on $\boldsymbol{\alpha}$, namely

$$\|\boldsymbol{\alpha}\|_p = 1 \quad \text{with} \quad \|\boldsymbol{\alpha}\|_p = (\textstyle\sum_{i=1}^{2} |\alpha_i|^p)^{1/p}. \tag{19}$$

For $p = 1$, Eq. (19) reduces to $\alpha_1 + \alpha_2 = 1$, while $p = 2$ yields the Euclidean norm. The parameter p therefore defines a family of admissible load combinations on which the minimum of $\lambda(\boldsymbol{\alpha})$ is sought.

Fig. 5 shows the isolines of $\lambda(\boldsymbol{\alpha})$ obtained by varying α_1 and α_2 between 0 and 1, the constraint curves associated with $p = 1, 2, 3, 5$ and 10, together with the minimum found for each constraint. Table 2 displays the load magnitudes pertaining to each p-norm. These results indicate that for $p = 1$ the minimum lies at (0, 1) (all load applied on the weakest member, the vertical bar 2), and increasing p shifts the solution toward the right (i.e. toward increasing α_1), while α_2 is always near 1. This is consistent with the fact that, as $p \to \infty$, the norm constraint approaches a max-type condition, which promotes load combinations where all components are at their maximum. Furthermore, the solution consistently favors a larger contribution from the vertical load (α_2) due to the fact that the vertical member has a lower bending stiffness, hence the load has a significant destabilizing effect.

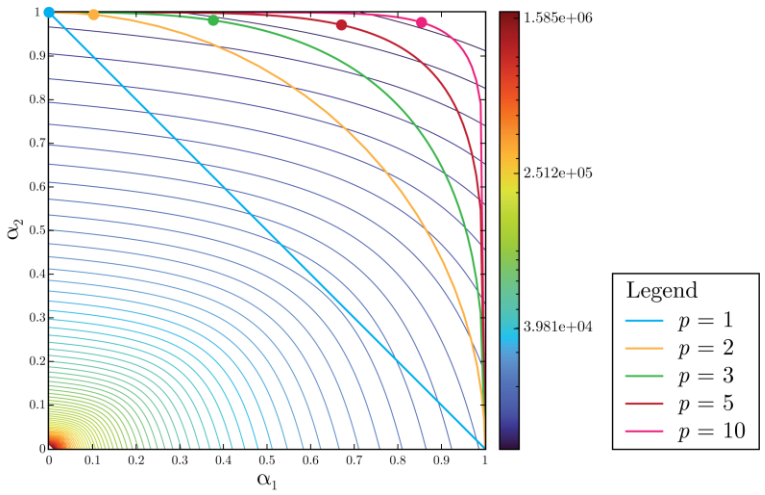

Figure 5: Inverted L-frame isolines for λ, p-norm constraints and minima for $p = 1, 2, 3, 5, 10$

Table 2: Inverted L-frame load magnitudes pertaining to the minimum critical load factor, for $p = 1, 2, 3, 5, 10$

p-norm	α_1	α_2
1	0	1
2	0.1025	0.9947
3	0.3768	0.9818
5	0.6708	0.9712
10	0.8544	0.9770

Fig. 6 shows the critical buckling mode shapes for $p = 1, 3$ and 10. A change in the mode shapes can be observed as p increases; the amplitudes of the deformed shapes in the two bars become progressively more similar. While for lower p the vertical bar exhibits a dominant deformed shape, increasing p leads to a gradual increase in the amplitude of the shape of the horizontal bar, so that both members contribute comparably to the critical mode. This trend is consistent with the corresponding load combinations, where larger p values promote solutions in which both load weights are simultaneously large.

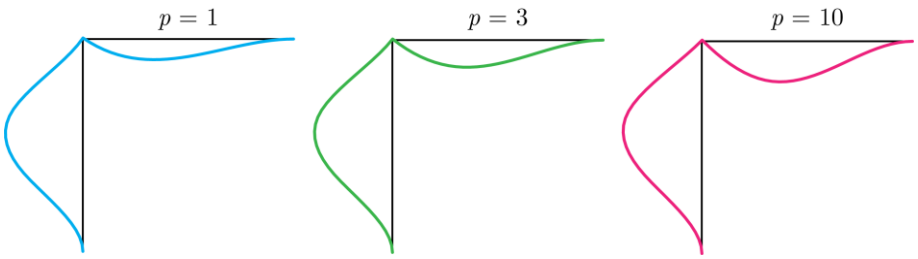

Figure 6: Inverted L-frame critical buckling mode shapes for $p = 1, 3, 10$

5.5 Braced non-sway frame

Consider the braced non-sway frame shown in Fig. 7. All members have equal length of 3 m and Young's modulus $E = 210$ GPa. The structure is subjected to two concentrated vertical loads applied at the top nodes and uniformly distributed loads acting on the left column and horizontal beam. The distributed load α_3 is scaled by a multiplier μ which can take the value of $+1$ or -1 depending on whether the load is directed to the right or to the left, respectively.

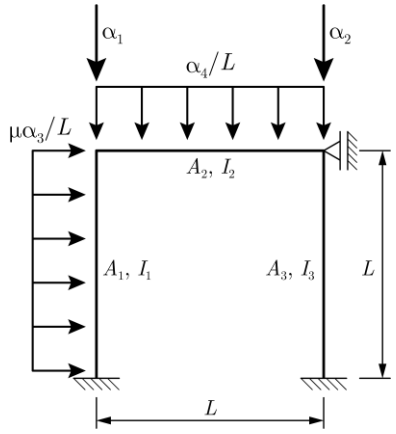

Figure 7: Braced non-sway frame with equal-length members

Consider the discrete case described in Section 4. For illustrative purposes, the leading load case is assigned with a multiplier equal to 1, whereas the remaining loads take discrete combination values equal to 0 or 0.7. The Genetic Algorithm was employed to solve the resulting discrete optimization problem using the following parameters:

- Population size: $P = 10$;
- Maximum number of generations: $G = 150$;
- Number of elite individuals retained per generation: $e = 2$;
- Tournament selection sample size: $t = 2$;
- Crossover probability: $p_c = 0.8$;
- Mutation probability of the leading-load gene: $p_{ml} = 0.05$;
- Mutation probability of the remaining genes: $p_{mr} = min\{0.05, 1/D\}$, where D is the number of genes.

As discussed previously, the algorithm terminates either when the maximum number of generations is reached or when the improvement in the best solution becomes negligible. Specifically, at generation g,

$$\left|\lambda^{(g)} - \lambda^{(g-k)}\right| < \varepsilon, \tag{20}$$

where $k = 20$ and $\varepsilon = 10^{-4}$.

Four cases were investigated by varying the distributed load multiplier μ and the second moment of area of the right column, namely:

A. $\mu = 1$, $I_1 = I_3 = 167.3$ cm^4, $I_2 = 317.5$ cm^4, $A_1 = A_3 = 26$ cm^2 and $A_2 = 34$ cm^2;
B. $\mu = -1$, same cross-section properties as Case A;
C. $\mu = 1$, $I_1 = 167.3$ cm^4, $I_2 = I_3 = 317.5$ cm^4, $A_1 = 26$ cm^2 and $A_2 = A_3 = 34$ cm^2;
D. $\mu = -1$, same cross-section properties as Case C.

The optimal load combinations and corresponding minimum critical load factors are summarized in Table 3, where the leading load in each case is highlighted in bold. Moreover, Fig. 8 shows the critical buckling mode shapes associated with each case.

Table 3: Optimal discrete load combinations and corresponding minimum critical load factors

Case	α_1	α_2	α_3	α_4
A	**1**	0.7	0.7	0.7
B	0.7	**1**	0.7	0.7
C	**1**	0.7	0.7	0.7
D	**1**	0.7	0	0.7

The results indicated that when the columns have identical stiffness (Cases A and B), the leading load corresponds to that applied directly to the column experiencing the highest compressive force. When the right column is stiffer than the left one (Cases C and D), the leading load is consistently α_1, reflecting the greater susceptibility of the slenderer column to buckling. In Case D the participation of the horizontal distributed load is zero because it introduces a slight traction in the critical column. The vertical distributed force is always detrimental and therefore always acts with the combination value.

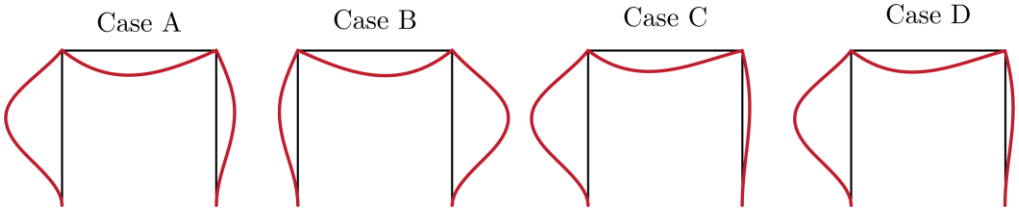

Figure 8: Braced non-sway frame critical buckling mode shapes for cases A-D

6. Conclusions

This paper addressed the problem of finding the load combination that minimizes the critical bifurcation load of elastic structures, which is of particular interest in structural optimization, for the identification of worst-case loading scenarios and assessing the sensitivity of structural stability to load variations. Two complementary problems were investigated. For continuously varying load case magnitudes subject to constraints, a gradient-based and closest-point projection strategy was proposed. The gradient corresponds to the eigenvalue sensitivities with respect to the magnitudes and provides valuable insight into the relative influence of each load case, allowing the identification of the "critical" member. For problems involving discrete load magnitudes, as

typically encountered in code-based limit state load combinations, a Genetic Algorithm was adopted instead.

The numerical examples presented concern 2D frame structures and lipped channel columns undergoing local/distortional buckling. These examples highlight the capability of the proposed methodologies to identify the most unfavorable load combinations and the "critical" members, and show potential for optimization methods in stability-aware structural design.

Acknowledgments
This research was funded in whole or in part by the Fundação para a Ciência e a Tecnologia, I.P. (FCT, https://ror.org/00snfqn58) under Grant UID/6438/2025 (https://doi.org/10.54499/UID/06438 /2025) of the research unit CERIS. For the purpose of Open Access, the author has applied a CC-BY public copyright license to any Author's Accepted Manuscript (AAM) version arising from this submission.

References

Bebiano, R., Gonçalves, R., Camotim, D. (2015). "A cross-section analysis procedure to rationalise and automate the performance of GBT-based structural analyses." *Thin-Walled Structures*, 92, 29-47.

Bebiano, R., Camotim, D., Gonçalves, R. (2018). "GBTUL 2.0 – a second-generation code for the GBT-based buckling and vibration analysis of thin-walled members." *Thin-Walled Structures*, 124 235-253.

Gonçalves R., Camotim D., Basaglia C., Martins A., Peres N. (2023). "Latest developments on the analysis of thin-walled structures using Generalised Beam Theory (GBT)." *Journal of Constructional Steel Research*, 204, 107858.

Courant, R., Hilbert, D. (1953). *Methods of mathematical physics*, Vol. 1, New York, Interscience Publishers.

Gholizadeh, S., Danesh, M., Gheyratmand, C. (2020). "A new Newton metaheuristic algorithm for discrete performance-based design optimization of steel moment frames." *Computers and Structures*, 234, 106250.

MATLAB, version R2024b, The MathWorks Inc., Massachusetts, 2024.

Murren, P., Khandelwal, K. (2014). "Design-driven harmony search (DDHS) in steel frame optimization." *Engineering Structures*, 59, 798-808.

Neves, M., Basaglia, C., Camotim, D., Araujo, H. (2024). "Improving the local and distortional resistance of CFS trapezoidal self-supporting roof members." *Thin-Walled Structures*, 201, 112054.

Przemieniecki, J. (1969). *Theory of Matrix Structural Analysis*, McGraw-Hill.

Saka, M. (2007). "Optimum design of steel frames using stochastic search techniques based on natural phenomena: a review", *Civil Engineering Computations: Tools and Techniques*, Saxe-Coburg, Stirlingshire, UK, 105-147.

Schardt, R. (1994). "Generalized beam theory — an adequate method for coupled stability problems." *Thin-Walled Structures*, 19(2), 161-180.

Togan V. (2012). "Design of planar steel frames using teaching-learning based Optimization." *Engineering Structures*, 34, 225-232.

Wittrick, W. (1962). "On eigenvalues of matrices dependent of a parameter." *Numerische Mathematik*, 6, 377-387

Ye, J., Hajirasouliha, I., Becque, J., Eslami, A. (2016). "Optimum design of cold-formed steel beams using Particle Swarm Optimisation method.", *Journal of Constructional Steel Research*, 122, 80-93.